Available online at www.sciencedirect.com
ScienceDirect
International Journal of Heat and Fluid Flow 28 (2007) 1060–1072
International Journal of HEAT AND FLUID FLOW
www.elsevier.com/locate/ijhff

Flow pattern based two-phase frictional pressure drop model for horizontal tubes, Part II: New phenomenological model

Jesús Moreno Quibén, John R. Thome *

Laboratory of Heat and Mass Transfer (LTCM), Faculty of Engineering Science (STI), École Polytechnique Fédérale de Lausanne (EPFL), CH-1015 Lausanne, Switzerland

Received 17 March 2006; received in revised form 10 January 2007; accepted 10 January 2007
Available online 19 April 2007

Abstract

This work presents an analytical investigation of two-phase pressure drops during evaporation in horizontal tubes. Based on a comprehensive state-of-the-art review and comparison with two-phase frictional pressure drop prediction methods, it is proven that none of these existing methods were adequate to predict the experimental values presented in Part I. Hence, an analytical study was undertaken in order to develop a new two-phase frictional prediction method. The new model has been developed following a phenomenological approach as the interfacial structure between the phases is taken into account. The recent [Wojtan, L., Ursenbacher, T., Thome, J. R., 2005a. Investigation of flow boiling in horizontal tubes: Part I – a new diabatic two-phase flow pattern map. Int. J. Heat Mass Transf. 48, 2955–2969] map was chosen to provide the corresponding interfacial structure. The new model treats each flow regime separately and then insures a smooth transition at the transition boundary, in agreement with the experimental observations. Next, based on a statistical comparison, it is concluded that the new two-phase frictional pressure drop flow pattern map based model successfully predicts the new experimental database and captures the numerous trends observed in the data.

Keywords: Two-phase flow; Two-phase pressure drops; Flow pattern maps; Flow regimes

1. Introduction

Despite numerous theoretical and experimental investigations, no general models are available that reliably predict two-phase pressure drops. A reason for this is that two-phase flow includes all the complexities of single-phase flows like non-linearities, transition to turbulence and instabilities plus additional two-phase characteristics like motion and deformation of the interface, non-equilibrium effects and interactions between phases. The prediction of this important design parameter is made by one of three approaches: empirical correlations, analytical models or phenomenological models. The main advantages and disadvantages of those approaches are:

1.1. Empirical

This is a commonly approach in modelling two-phase pressure drop (see Lockhart and Martinelli, 1949; Bankoff, 1960; Cicchitti et al., 1960; Thom, 1964; Pierre, 1964; Baroczy, 1965; Chawla, 1967; Chisholm, 1973; Friedel, 1979; Grönnerud, 1979; Müller-Steinhagen and Heck, 1986). The main reason in following this approach is that minimum knowledge of the flow characteristics is required. Thus, empirical models are easy to implement and often they provide good accuracy in the range of the database available for the development of the correlation. As a consequence, one of principal disadvantages of this approach is that they are limited by the range of their underlying

* Corresponding author. Tel.: +41 21 693 54 41; fax: +41 21 693 59 60.
E-mail addresses: jesus.moreno@epfl.ch (J. Moreno Quibén), john.thome@epfl.ch (J.R. Thome).

0142-727X/$ - see front matter
doi:10.1016/j.ijheatfluidflow.2007.01.004

database. Another important disadvantage of the empirical approach is that no single correlation is currently able to provide an acceptable accuracy for general use.

1.2. Analytical

Two-phase pressure drop models developed following this approach are general models since no empirical information is used in their development. Besides this obvious positive aspect, the corresponding mathematical models are very complex and often iterative and numerical procedures are required resulting in time consuming calculations. In addition, these methods in two-phase flow require difficult to obtain data for their validation.

1.3. Phenomenological

Two-phase pressure drop models developed following a phenomenological approach are theoretical based methods as the interfacial structure is taken into account (see Bandel, 1973; Beattie, 1972; Hashizume et al., 1985; Olujić, 1985 and Hart et al., 1989). Thus, they are not blind to the different flow regimes resulting in general applicability models. Despite this obvious advantage, an important drawback of this approach is that some empiricism is still required in order to close the model. Another important aspect is that no general flow pattern based model is yet available. In fact, phenomenological models are typically only available for individual flow patterns or flow structures. This observation preludes one of the major difficulties in following this approach, that is they need a very reliable flow pattern map in order to be able predict the different interfacial structures and the transitions from one regime to another.

2. Comparison to existing methods

Tribbe and Müller-Steinhagen (2000) compared some of the leading two-phase frictional pressure drop correlations to a large database, including the following fluid combinations: air–oil, air–water, water–steam and several refrigerants. They found that statistically the method of Müller-Steinhagen and Heck (1986) gave the best and most reliable results. In another recent comparison, Ould-Didi et al. (2002) compared leading methods to experimental pressures drops obtained for five different refrigerants over a wide range of experimental conditions. Overall, they found the Grönnerud (1979) and the Müller-Steinhagen and Heck methods to be equally best, while the Friedel (1979) method was the third best in a comparison to seven leading methods.

As a first step in the present analysis, the experimental results were compared to the three previously "best" methods. The popular Lockhart–Martinelli correlation is not shown here in this comparison in spite of its extensive use and continued historical references because it was not well ranked in previous studies (nor does it compare well to the present data).

Fig. 1 shows a representative comparison of the three prediction methods (Friedel, Grönnerud and Müller-Steinhagen and Heck) for different experimental conditions. Starting first with the Grönnerud method, it works quite well at low mass velocities from low to medium vapor qualities and it also predicts a maximum as in the data at high vapor quality, although not necessarily its magnitude but reasonably well the location of the peak. Instead, at the highest mass velocities tested the Grönnerud method significantly overpredicts all the results except at low vapor qualities. The Müller-Steinhagen and Heck correlation does not follow the trends in the data well, underpredicting most of them and does not capture the peak in the data. The Friedel method is seen to predict values similar to those of Müller-Steinhagen and Heck. For the sake of simplicity, comparisons for refrigerant R134a are not shown here but the situation is essentially the same.

Fig. 2 shows a comparison of the complete database to the three prediction methods (Friedel, Grönnerud and Müller-Steinhagen and Heck). Certainly of the three, the Müller-Steinhagen and Heck comes out the best overall. However, it is only able to predict one-half of the database within $\pm 20\%$. Hence, it is clear that none of these three methods are reliable for optimizing the thermal-hydraulics of a direct-expansion evaporator, eventhough statistically they are not that bad when considering the normal situation for the prediction of two-phase frictional pressure drops.

3. Limitations of existing methods

In general, the existing two-phase frictional pressure models available in the literature for horizontal flows have some or all of the following deficiencies:

- They do not account for flow pattern effects on the process, which are particularly important at low flow rates (stratification effects) and at high vapor qualities (dryout effects).
- They do not account explicitly for the influence of interfacial waves.
- They do not account for the upper dry perimeter of stratified types of flows.
- They do not use the actual velocities of the vapor and liquid by introduction of the local void fraction into the method.
- They use tubular flow expressions to represent annular film flows.
- They do not capture the peak in the pressure gradient at high vapor qualities (or not its location or magnitude) nor give a good representation of the pressure gradient trend versus vapor quality.
- They do not go to acceptable limits at $x = 0$ and $x = 1$.

Hence, this state of affairs is the justification to develop a new model. Secondly, the present flow pattern based pressure drop model fits into the unified method of Thome and

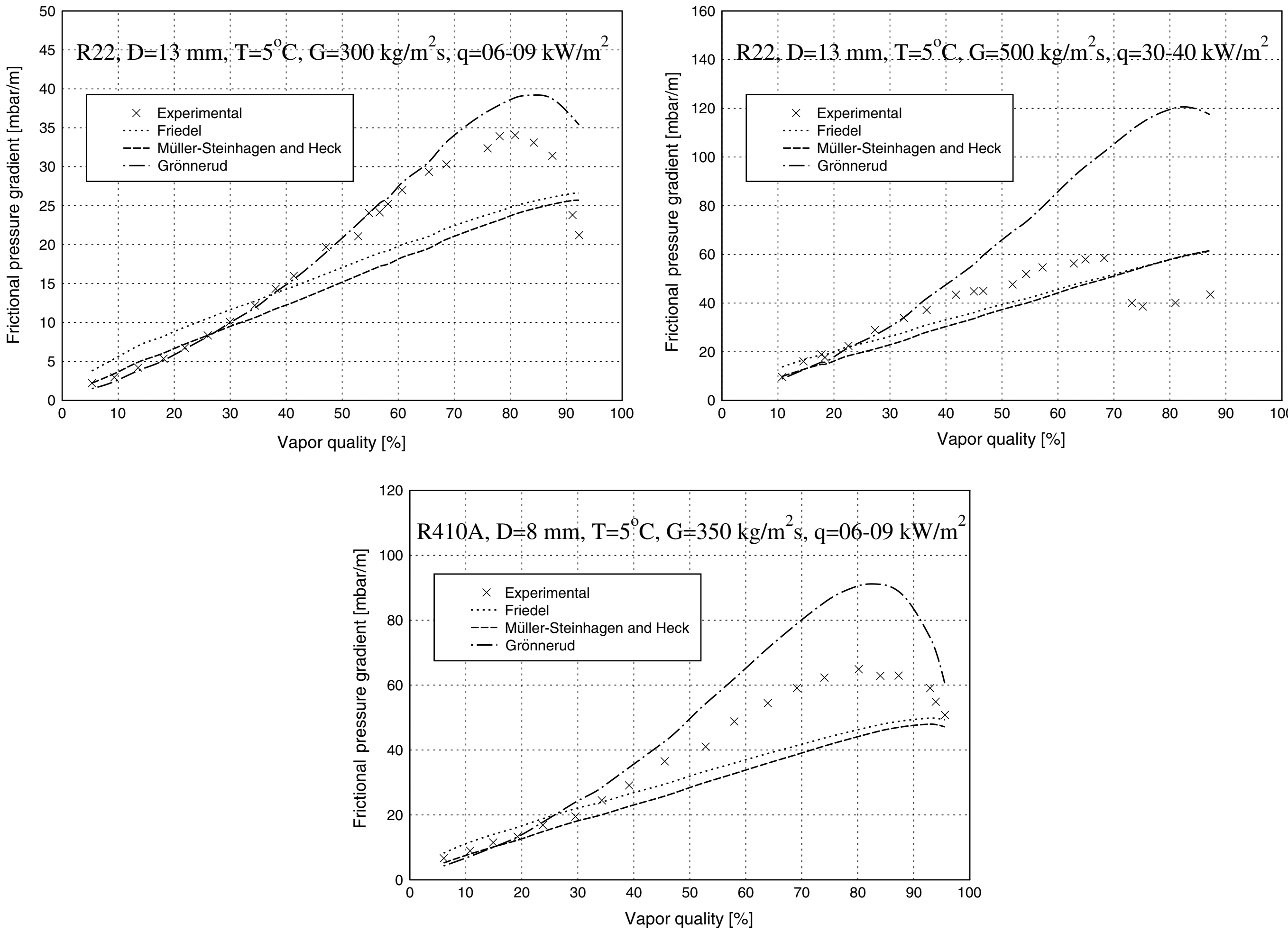

Fig. 1. Frictional pressure gradients vs. three prediction methods for R22 and R410A at different experimental conditions.

coworkers to model evaporation (Wojtan et al., 2005a,b) and condensation (el Hajal et al., 2003a,b) inside horizontal tubes.

4. New two-phase pressure drop model

4.1. Introduction

The new two-phase frictional pressure drop model is developed following a phenomenological approach, that is physically based on several simplified interfacial two-phase flow structures. The corresponding interfacial flow structures are determined using the recent (Wojtan et al., 2005a) flow pattern map.

4.2. Segregation of experimental data by flow pattern

Table 1 shows the entire database segregated by flow regime using the recent Wojtan et al. flow pattern map. It has to be pointed out here that only experimental values where the complete test section was in the same flow regime are taken into account. This restriction is always verified for the adiabatic test section as no heat is added to the refrigerant, while for the diabatic test section the inlet and outlet vapor qualities were checked to verify that the entire test section was in the same regime. For this reason only 1745 experimental points have been used in new model development from the 2543 values obtained (representing about 50% diabatic data and 50% adiabatic data).

It has to be pointed out here that the fixed value of the mass velocity appearing in the graphs depicted in Fig. 3 represents the value used for the void fraction calculation using Steiner (1993) version of the Rouhani and Axelsson (1970) drift flux model

$$\epsilon = \frac{x}{\rho_G}\left[(1+0.12(1-x))\left(\frac{x}{\rho_G}+\frac{(1-x)}{\rho_L}\right) + \frac{1.18(1-x)[g\sigma(\rho_L-\rho_G)]^{0.25}}{G\rho_L^{0.5}}\right]^{-1} \quad (1)$$

As the variation of this value practically does not affect the void fraction calculation for mass velocities above 50 kg/m^2 s, a design condition for the mass velocity is assumed for simplicity in generating these graphs and this is the value appearing in the title of the graphs. In actual

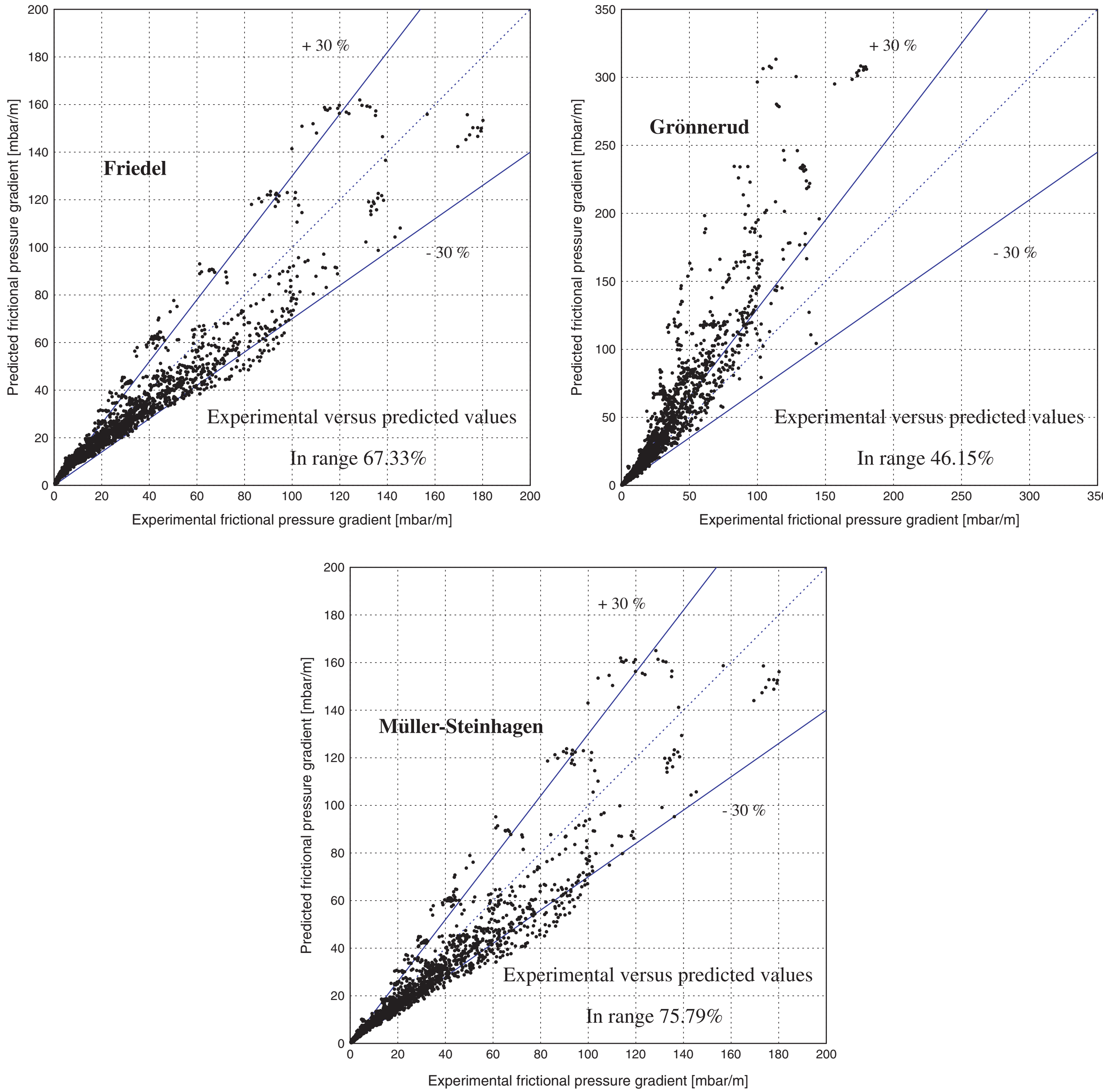

Fig. 2. Comparisons of experimental to predicted values using Friedel, Grönnerud, and Müller-Steinhagen and Heck correlations against the entire database.

Table 1
Segregated experimental values by flow regime using Wojtan et al. flow pattern map

Segregated experimental values by flow regime									
Fluid	D (mm)	Slug + SW	SW	Slug	I	A	D	M	S
R134a	13.8	6	3	5	2	13	0	0	0
R22	8	28	20	18	12	75	21	17	0
R22	13.8	18	54	15	37	162	44	47	0
R410A	8	26	19	24	55	167	121	110	0
R410A	13.8	78	115	17	77	166	104	69	0
Total		156	211	79	183	583	290	243	0

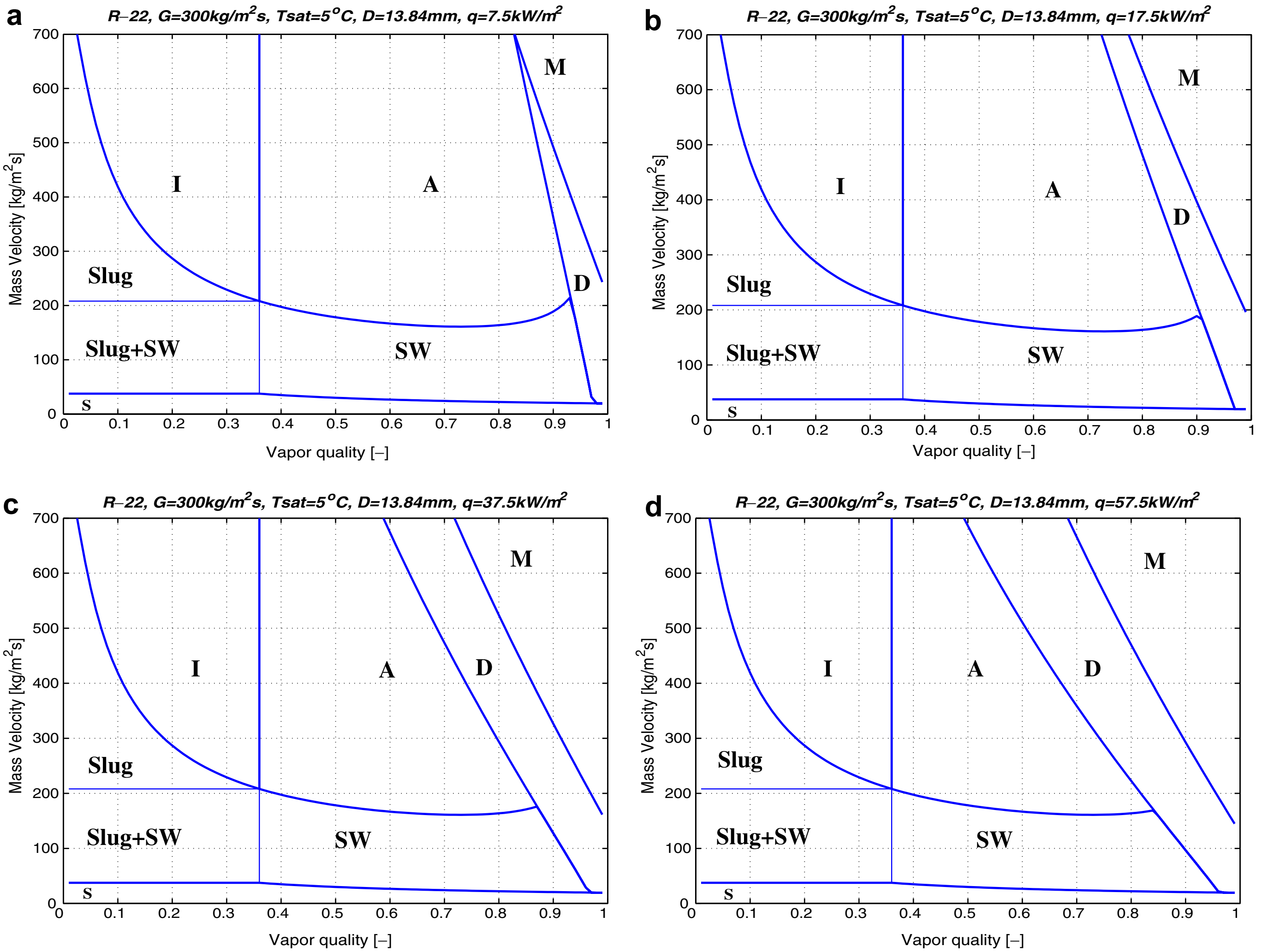

Fig. 3. Flow pattern maps for R-22, $T_{sat} = 5\ °C$, $D = 13.84$ mm at $G = 300\ \ kg/m^2s$ and heat fluxes: (a) 7.5 kW/m^2, (b) 17.5 kW/m^2, (c) 37.5 kW/m^2 and (d) 57.5 kW/m^2.

application of the flow pattern map and the new frictional pressure drop model, the actual mass velocity is used in calculations.

4.3. Model development

Once the flow regime is known, a simplified interfacial structure can be assumed, and then a set of equations is proposed to determine the two-phase pressure drop for that regime, while at the same time taking care not to have any jumps in the predicted values when crossing a flow transition boundary. Below, the new model and its calculation procedure for the different flow regimes is proposed and described.

4.3.1. Annular region (A)

According to the flow pattern map, about one-third of the experimental data were in the annular flow regime. Therefore, this regime will be treated first. The model for analysis is a simplified annular flow structure consisting of a liquid film and a gas core, as shown Fig. 4. Entrainment is neglected and the liquid film is assumed to have a uniform thickness δ around the circumference. These assumptions are not always valid but they allow a much more simplified model to be proposed.

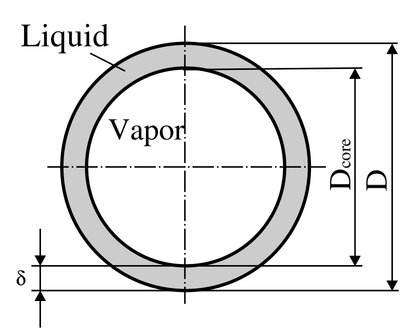

Fig. 4. Simplified annular flow configuration.

The model is based on the steady-state gas and liquid phase momentum balance equations. Assuming equal average pressure gradients in the gas and liquid, which is generally valid in the absence of interfacial liquid level gradients, this leads to the following equation:

$$\frac{\Delta p}{L} = 4\frac{\tau_i}{(D-2\delta)} \tag{2}$$

Taking into account that generally $D \gg \delta$, Eq. (2) can be written as follows:

$$\frac{\Delta p}{L} = 4\frac{\tau_i}{D} \tag{3}$$

The expression above states that the frictional pressure gradient is directly related to the interfacial shear stress τ_i and the tube diameter D. The interfacial shear stress represents the shear stress exerted by the gas on the liquid and is given by

$$\tau_i = f_i\frac{1}{2}\rho_G(u_G-u_L)^2 \approx f_i\frac{1}{2}\rho_G u_G^2 \quad \text{if} \quad u_L \ll u_G \tag{4}$$

where f_i is the interfacial friction factor and u_G and u_L are the true average velocities calculated with the following expressions

$$u_G = \frac{G}{\rho_G}\frac{x}{\epsilon} \tag{5}$$

$$u_L = \frac{G}{\rho_L}\frac{1-x}{1-\epsilon} \tag{6}$$

The interfacial friction factor f_i remains unknown and is as always the most difficult parameter to model in two-phase flow. From Eqs. (3) and (4) and the present two-phase frictional pressure drop database in the annular flow regime obtained during the experimental campaign used to give a data set for f_i, the following new film flow correlation for f_i is proposed

$$(f_i)_{\text{annular}} = 0.67\underbrace{\left[\frac{\delta}{2R}\right]^{1.2}}_{1}\underbrace{\left[\frac{(\rho_L-\rho_G)g\delta^2}{\sigma}\right]^{-0.4}}_{2}\underbrace{\left[\frac{\mu_G}{\mu_L}\right]^{0.08}}_{3}\underbrace{[We_L]^{-0.034}}_{4} \tag{7}$$

where the non-dimensional groups include the following effects

- 1: Film thickness effect relative to the internal radius of the tube R, where the film thickness is calculated by means of the following equation:

$$\delta = \frac{A_L}{R(2\pi-\theta\text{dry})} = \frac{A(1-\epsilon)}{R(2\pi-\theta_{\text{dry}})} = \frac{\pi D(1-\epsilon)}{2(2\pi-\theta_{\text{dry}})} \tag{8}$$

  with $\theta_{\text{dry}} = 0$ for annular flow.
- 2: This expression comes from manipulation of the Helmholtz instability equation using δ as the scaling factor for the most dangerous wavelength for the formation of interfacial waves.
- 3: The viscosity ratio of the gas and liquid phases.
- 4: The liquid Weber We_L calculated using the following expression:

$$We_L = \frac{\rho_L u_L^2 D}{\sigma} \tag{9}$$

The empirical constant and exponents were obtained statistically from the annular flow database. Hence, the frictional two-phase pressure drop can be now calculated with:

$$(\Delta p)_{\text{annular}} = 4(f_i)_{\text{annular}}\left(\frac{L}{D}\right)\frac{\rho_G u_G^2}{2} \tag{10}$$

4.3.2. Slug + Intermittent (Slug + I)

These two flow regimes were treated together as noted in Table 1 since their respective experimental frictional two-phase pressure drops follow similar trends in Figs. 12–14 in Part I. This behaviour is consistent with the Wojtan (2004) observations regarding flow boiling heat transfer coefficients. Moreover, due to the unsteadiness of the flow characterizing these two regimes, trying to capture this behaviour is quite complex. A common characteristic of both regimes is that all the tube perimeter is continuously wetted, explaining perhaps why their data have similar trends.

For the reasons mentioned above, and to avoid a jump at the transition with annular flow while also respecting the natural limit at $x = 0$, a good compromise was found by using the following expression:

$$(\Delta p)_{\text{slug+intermittent}} = \Delta p_{L0}\left(1-\frac{\epsilon}{\epsilon_{IA}}\right)^{0.25} + (\Delta p)_{\text{annular}}\left(\frac{\epsilon}{\epsilon_{IA}}\right)^{0.25} \tag{11}$$

where Δp_{L0} is single-phase frictional liquid pressure drop (evaluated at $x = 0$), ϵ_{IA} is the void fraction at the intermittent to annular transition boundary x_{IA} and $(\Delta p)_{\text{annular}}$ is the two-phase frictional pressure drop evaluated at the actual vapor quality using the annular flow equations and Eq. (8) with $\theta_{\text{dry}} = 0$ to calculate the corresponding film thickness.

Eq. (11) is an interpolation between the single-phase frictional liquid pressure drop ($x = 0$) and the two-phase frictional pressure drop $(\Delta p)_{\text{annular}}$ that would exist if the regime were annular for these flow conditions. Using the void fraction in the interpolation procedure, this expression accomplishes two important purposes: first, it matches the correct limit at $x = 0$ (single-phase liquid flow), and second it insures a smooth transition at the intermittent to annular transition without introducing any jump. In doing so, the model is in agreement with the experimental observations and bypasses these two drawbacks of some existing models.

4.3.3. Stratified-wavy (SW)

In this regime, the parameter that defines the flow structure and the ratio of the tube perimeter in contact with the liquid and gas is the dry angle θ_{dry} shown in Fig. 5.

It is an experimental fact that in stratified-wavy flow that liquid creeps up the sides of the tube to a varying extend. This effect significantly affects the interfacial perimeters P_i,

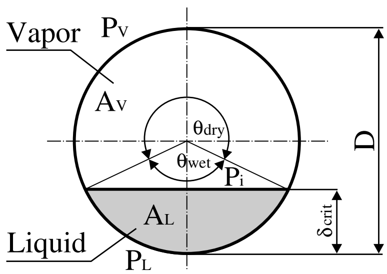

Fig. 5. Simplified stratified flow configuration.

P_L and P_G, as well as the interfacial friction factor f_i. In fact, for a fixed vapor quality x, θ_{dry} varies from 0 for $G_{wavy}(x)$ at the annular flow transition and to its maximum value of θ_{strat} for $G_{strat}(x)$ at the fully stratified flow transition. Several expressions have been proposed to capture this variation: a linear variation by Kattan et al. (1998) and a quadratic interpolation el Hajal et al. (2003b). In the recent work of Wojtan et al. (2005b) based on experimental heat transfer data for this region, they have proposed the following expression:

$$\theta_{dry} = \left[\frac{(G_{wavy} - G)}{(G_{wavy} - G_{strat})}\right]^{0.61}\theta_{strat} \tag{12}$$

where θ_{strat} is determined using the approximate expression for the implicit geometrical expression arising from Fig. 5, evaluated in terms of void fraction, proposed by Biberg (1999),

$$\theta_{strat} = 2\pi - 2\left\{\begin{array}{l}\pi(1-\epsilon) + \left(\frac{3\pi}{2}\right)^{1/3}[1-2(1-\epsilon)+(1-\epsilon)^{1/3}-\epsilon^{1/3}] \\ -\frac{1}{200}(1-\epsilon)\epsilon[1-2(1-\epsilon)][1+4((1-\epsilon)^2+\epsilon^2)]\end{array}\right\} \tag{13}$$

Using Eqs. (12) and (13) to determine θ_{dry}, the following equation is now proposed for the two-phase friction factor:

$$(f_{tp})_{stratified\text{-}wavy} = \theta^*_{dry} f_G + (1-\theta^*_{dry})(f_i)_{annular} \tag{14}$$

where $\theta^*_{dry} = \theta_{dry}/2\pi$, f_G is the single-phase gas friction factor calculated using the classical definition

$$f_G = \frac{0.079}{Re_G^{0.25}} \quad \text{where} \quad Re_G = \frac{GxD}{\mu_G \epsilon} \tag{15}$$

and $(f_i)_{annular}$ is the interfacial friction factor for the annular flow regime described previously evaluated at the actual vapor quality and using Eq. (8) to determine the corresponding film thickness. The frictional two-phase pressure drop can now be calculated as follows:

$$(\Delta p)_{stratified\text{-}wavy} = 4(f_{tp})_{stratified\text{-}wavy}\left(\frac{L}{D}\right)\frac{\rho_G u_G^2}{2} \tag{16}$$

4.3.4. Slug + Stratified-Wavy (Slug + SW)

In this regime both low amplitude waves (which do not reach the top of the tube) and liquid slugs washing the top of the tube are observed. With increasing vapor quality in this zone, the frequency of slugs decreases and the waves become more dominant. This behavior is highly chaotic and as a consequence is quite difficult to capture physically within a simplified model. A good compromise was found, as for the slug and intermittent regimes, by using the following expression:

$$(\Delta p)_{slug+SW} = \Delta p_{L0}\left(1 - \frac{\epsilon}{\epsilon_{IA}}\right)^{0.25} + (\Delta p)_{stratified\text{-}wavy}\left(\frac{\epsilon}{\epsilon_{IA}}\right)^{0.25} \tag{17}$$

where Δp_{L0} is the single-phase frictional liquid pressure drop (evaluated at $x = 0$), ϵ_{IA} is the void fraction at the intermittent to annular transition boundary and $(\Delta p)_{stratified\text{-}wavy}$ is the two-phase frictional pressure drop evaluated at the actual vapor quality using stratified-wavy flow equations. For this flow pattern, the following expression, proposed by el Hajal et al. (2003b), is used for the film thickness determination,

$$\delta = \frac{D}{2} - \sqrt{\left(\frac{D}{2}\right)^2 - \frac{2A_L}{(2\pi - \theta_{dry})}} \tag{18}$$

and it has been pointed out by Wojtan et al. (2005b) that when liquid occupies more than one-half of the cross-section of the tube at low vapor quality, this expression would yield a value of $\delta > D/2$, what is not geometrically realistic. Hence, whenever Eq. (18) gives $\delta > D/2$, δ is set to $D/2$. Eq. (17) again insures a smooth transition at the intermittent to annular boundary and matches the correct limit for $x = 0$. The interpolation exponent is again 0.25 as in Eq. (11) and gives the best representation of the data.

4.3.5. Mist (M)

This regime is encountered when all the liquid is entrained in the gas core by the high velocity gas. The vapor phase is the continuous phase and the liquid flows in the form of droplets. In fact, it is not far from reality to consider the two phases to flow as a single phase possessing mean fluid properties. Under these conditions one can use the homogeneous flow theory in order to predict two-phase frictional pressure drop values. Hence, the following expression is used to calculate the two-phase frictional pressure drop in this regime:

$$(\Delta p)_{mist} = 2f_m\left(\frac{L}{D}\right)\frac{G^2}{\rho_m} \tag{19}$$

where ρ_m is the homogeneous density determined as

$$\rho_m = \rho_L(1-\epsilon_H) + \rho_G\epsilon_H \tag{20}$$

and the homogeneous void fraction ϵ_H is

$$\epsilon_H = \frac{1}{1 + \frac{(1-x)}{x}\frac{\rho_G}{\rho_L}} \tag{21}$$

The friction factor f_m is calculated introducing the homogeneous viscosity μ_m using single-phase equations as follows,

$$f_m = \frac{0.079}{Re_m^{0.25}} \quad \text{where} \quad Re_m = \frac{GD}{\mu_m} \tag{22}$$

and μ_m is determined using Cicchitti et al. (1960) expression:

$$\mu_m = x\mu_G + (1-x)\mu_L \tag{23}$$

This expression (Eq. (19)) goes to the ideal limit of all gas flow at $x = 1$.

4.3.6. Dryout (D)

Analyzing the experimental results, it is obvious that there is not usually a step-wise jump in the frictional pressure gradient from annular (A) to mist (M) flow. This transition regime between them is called dryout. The process of dryout starts at the top of the tube, where the liquid film is thinner, and takes place over a range of vapor quality (from the inception of dryout at x_{di} at the top of the tube to the completion of dryout at x_{de} at the bottom of the tube) and thus ends when the fully developed mist flow regime is reached. This process is depicted in Fig. 6.

The following linear interpolation captures this variation and does not introduce any jump in the frictional pressure gradient, being in agreement with the experimental observations

$$(\Delta p)_{dryout} = (\Delta p)_{tp}(x_{di}) - \frac{x - x_{di}}{x_{de} - x_{di}}[(\Delta p)_{tp}(x_{di}) - (\Delta p)_{mist}(x_{de})] \tag{24}$$

where x_{de} is the dryout completion quality and x_{di} is the dryout inception quality calculated according to the flow pattern map using expressions proposed by Wojtan et al. (2005b), $(\Delta p)_{tp}(x_{di})$ is the frictional pressure drop at the inception quality calculated either with Eq. (10) for annular flow or Eq. (16) for stratified-wavy flow and $(\Delta p)_{mist}(x_{de})$ is the frictional pressure drop at the completion quality calculated with Eq. (19). At high mass velocities the value of x_{de} intersects that of x_{di}; at these conditions, the dryout zone (D) no longer exits as all the liquid is thought to be stripped from the wall and a jump is contemplated between annular and mist flow.

4.3.7. Stratified (S)

The stratified flow regime was out of the possibilities of the present test facility as it occurs at very low mass velocities. Thus, no experimental values were obtained in this regime. In spite of no experimental verification, the following calculation procedure is proposed for this regime:

- if $x \geqslant x_{IA}$ then

$$(f_{tp})_{stratified} = \theta^*_{strat} f_G + (1 - \theta^*_{strat})(f_i)_{annular} \tag{25}$$

where $\theta^*_{strat} = \theta_{strat}/2\pi$, f_G is single-phase gas friction factor calculated with Eq. (15) and $(f_i)_{annular}$ is the interfacial friction factor for the annular flow regime described previously evaluated at the actual vapor quality.The frictional two-phase pressure drop can now be calculated as follows:

$$(\Delta p)_{stratified(x\geqslant x_{IA})} = 4(f_{tp})_{stratified}\left(\frac{L}{D}\right)\frac{\rho_G u_G^2}{2} \tag{26}$$

- if $x < x_{IA}$ then

$$(\Delta p)_{stratified(x<x_{IA})} = \Delta p_{L0}\left(1 - \frac{\epsilon}{\epsilon_{IA}}\right)^{0.25} + (\Delta p)_{stratified(x\geqslant x_{IA})}\left(\frac{\epsilon}{\epsilon_{IA}}\right)^{0.25} \tag{27}$$

where Δp_{L0} is single-phase frictional liquid pressure drop (at $x = 0$), ϵ_{IA} is the void fraction at the intermittent to annular transition boundary and $(\Delta p)_{stratified(x\geqslant x_{IA})}$ is the two-phase frictional pressure drop evaluated at the actual vapor quality using stratified flow equations for $x \geqslant x_{IA}$.

4.3.8. Bubbly (B)

Bubbly flows are not addressed here as these occur at very high mass velocities that are beyond the range of present interest. The bubbly flow transition from intermittent flow remains the same as in the original map (see Wojtan et al., 2005a).

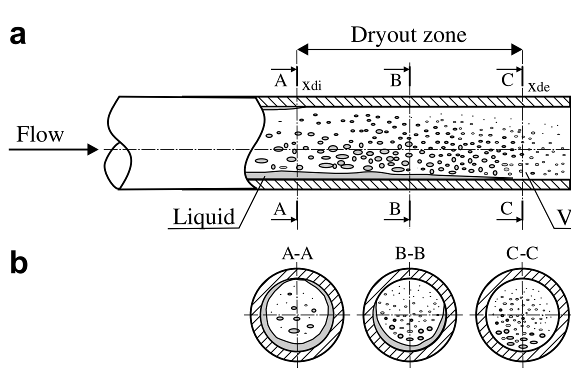

Fig. 6. Dryout zone during evaporation in horizontal tube.

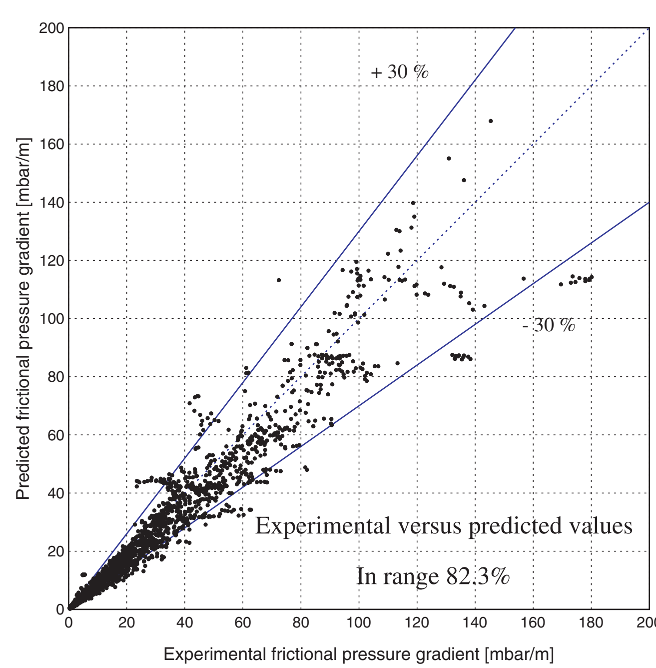

Fig. 7. Comparisons of experimental to predicted values for the entire database.

Table 2
Compilation of percentages of the database within an specific range for the new proposed model and three existing methods

Compilation of statistical results	±30%	±20%
Friedel	67.33%	51.81%
Grönnerud	46.15%	40.45%
Müller-Steinhagen and Heck	75.79%	49.64%
New method	82.30%	64.71%

5. Comparison of new model to database

This section presents comparisons of experimental to predicted values obtained using the new two-phase frictional pressure drop model.

Fig. 7 depicts comparisons of the entire database to predicted values. The new method predicts 82.3% within ±30% and 64.71% within ±20%. Taking into account that the

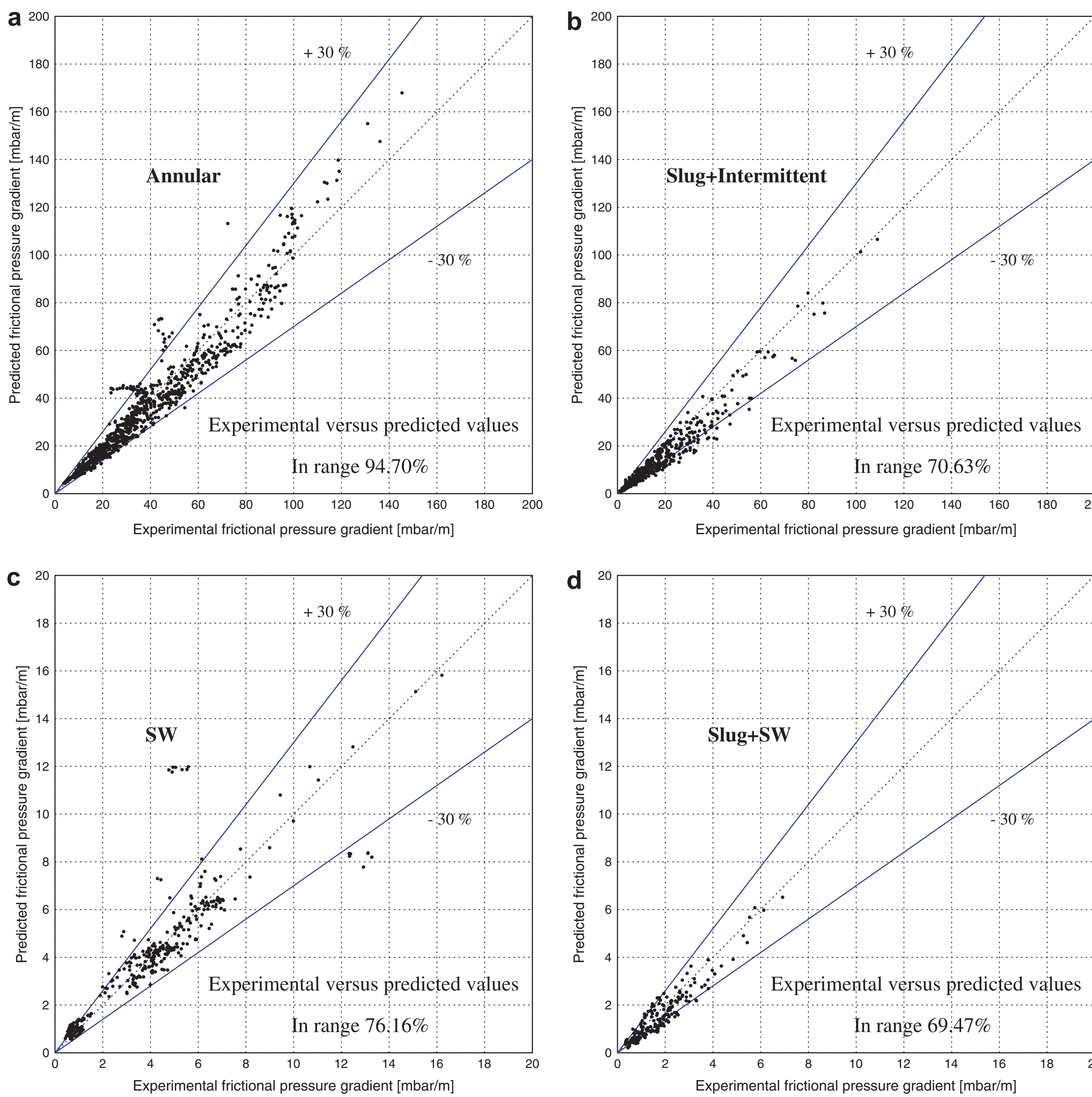

Fig. 8. Comparisons of experimental to predicted values for the entire database segregated by flow regime: (a) annular, (b) Slug + Intermittent, (c) SW and (d) Slug + SW.

range of experimental conditions included a wide range of experimental conditions (fluids, diameter, mass velocities, heat fluxes), the method predicts very accurately the experimental data. The values for all the database versus the new and previous methods are summarized in Table 2.

In order to check the reliability of the new model (Moreno Quibén, 2005) performed comparisons of experimental to predicted values when the fluid and diameter are changed and it is shown that changing these two important parameters does not have an effect on the accuracy of the predictions attesting for the reliability of the new method.

As the new frictional two-phase pressure drop model is flow pattern based, Fig. 8 shows comparisons of experimental to predicted values for the entire database segregated by flow regime. For the sake of simplicity, the mist and dryout results are not shown in this figure but a similar behavior was observed. It has to be pointed that pressure drop experimental values in the stratified-wavy (SW) and slug + stratified-wavy (Slug + SW) regimes were in the range of 0–8 m bar and trying to accurately predict such low values is a difficult task, because small deviations can induce large errors. Furthermore, the accuracy of identifying the flow pattern depends on the flow pattern map and hence test conditions near transitions can be wrongly predicted. In addition, since the fall off in the frictional pressure gradient after the peak at high vapor qualities is very dependent on the prediction of x_{di}, a small error in the latter has a magnifying effect on the former.

Thus, it has been shown that the new two-phase frictional prediction model from a statistical point of view is able to accurately predict the experimental values. The reliability of the proposed model has also been proven but still a question remains open: Does the new model capture the trends observed in the two-phase frictional pressure drops versus vapor quality? This latter issue is crucial for the thermal optimization of evaporators and is addressed below.

Figs. 9 and 10 show experimental and predicted values plotted versus quality for a selected set of experimental conditions. The new model follows the experimental trends quite well and it is able to capture reasonably well the position and a little less so the magnitude of the characteristic peak at high vapor qualities. Furthermore, in thermal design with a vapor quality change from $x = 0.2$ at the inlet to $x = 1$ at the outlet, it is most important that the two-phase pressure gradient is calculated accurately where the gradients are high. For example, a 20% error at $x = 0.2$ is

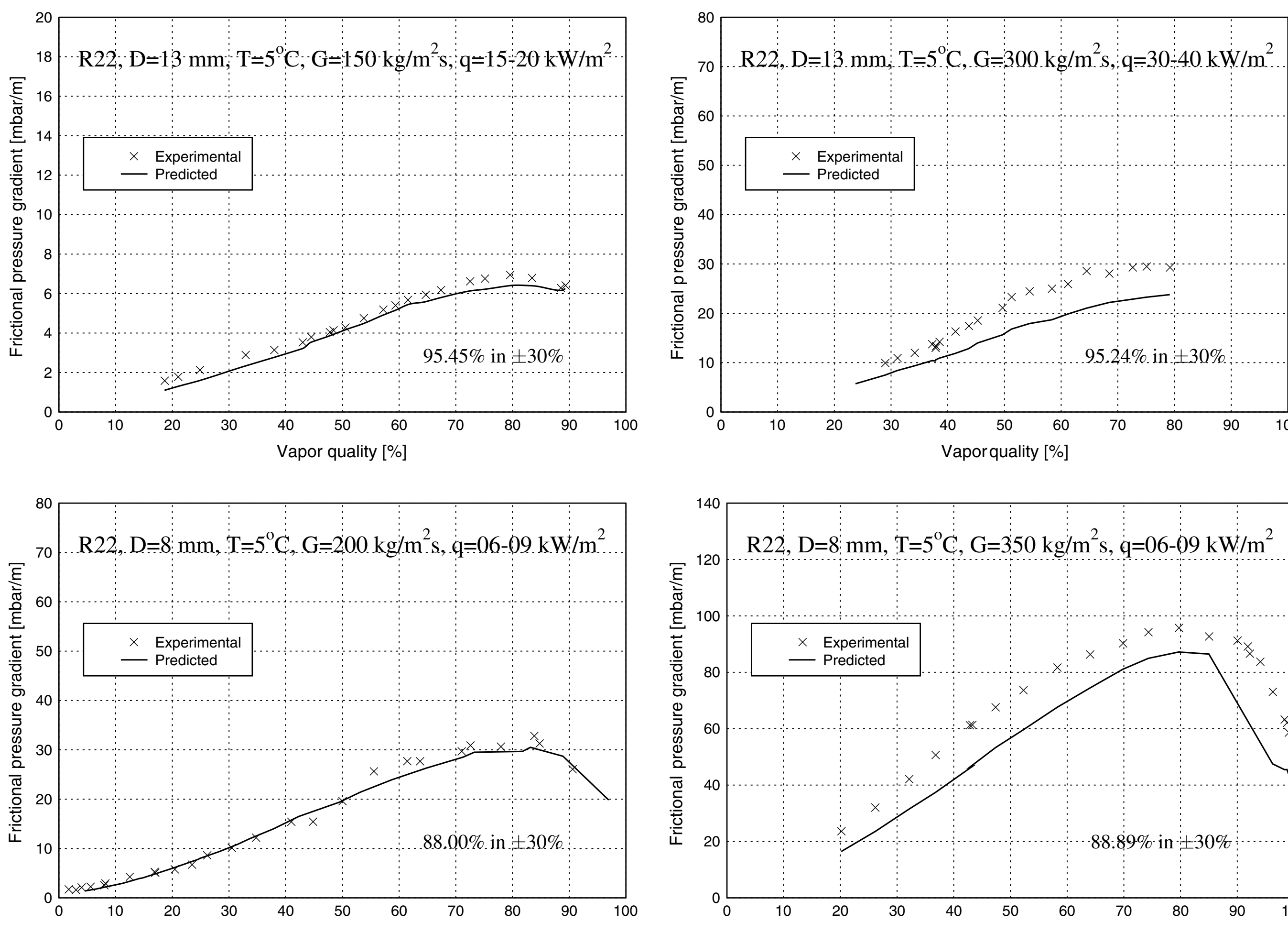

Fig. 9. Experimental and predicted values versus vapor quality for R22 at different experimental conditions.

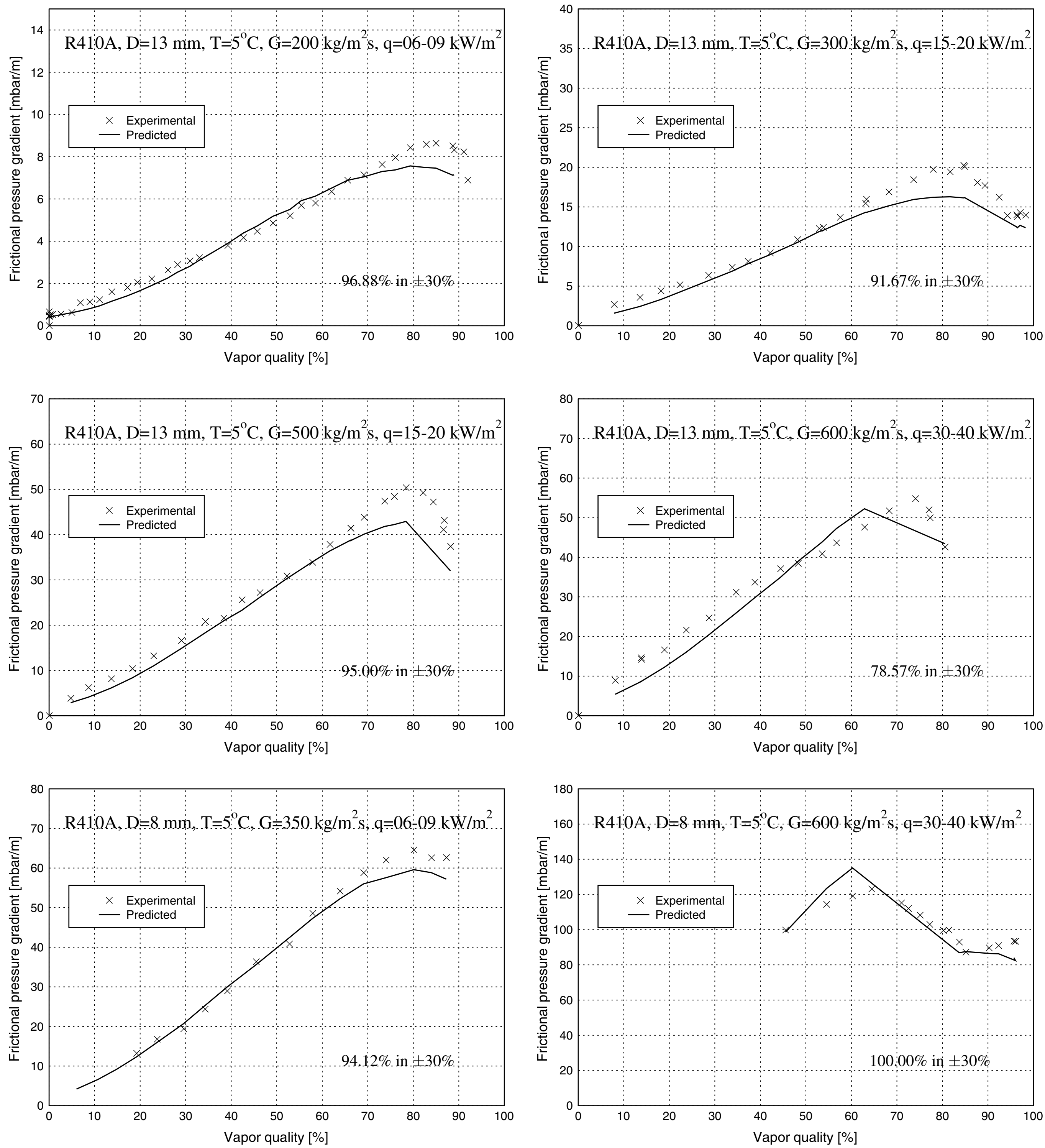

Fig. 10. Experimental and predicted values versus vapor quality for R410A at different experimental conditions.

insignificant in the total pressure drop calculation. Hence, the present method that works very well in annular flow (see Fig. 8a) and that captures the position of the peak will give much better total pressure drop predictions than the other methods.

Comments on the attributes of the new flow pattern based method are as follows:

- It is more accurate (according to Table 2) than the best competing methods.
- It better follows the variation in pressure gradient with vapor quality.
- It captures the peak in the pressure gradient at high vapor qualities.
- It handles mist flow and the dryout region.

- It goes to the correct limits at $x = 0$ (single-phase liquid flow) and at $x = 1$ (single-phase gas flow).
- It explicitly includes the effect of interfacial waves.
- It includes the effect of interfacial flow structure (such as partially dry perimeter) via the flow pattern map.
- It is based on the actual mean velocities of the phases via the void fraction equation rather than superficial velocities.

6. Conclusions

The experimental results presented in Part I were compared to three recommended two-phase frictional pressure drop correlations: Friedel, Grönnerud, and Müller-Steinhagen and Heck. While, all three provided a reasonable agreement for some particular set of experimental conditions, they either significantly overpredicted or underpredicted the data for most of the others. Also, the methods did not reliably capture the variation in two-phase frictional pressure drop versus vapor quality, which is necessary for such methods to be useful for the thermal optimization of evaporators. Hence, the development of new two-phase frictional pressure drop model based on flow pattern map is justified. Then, the experimental data were segregated by flow regime using the recent Wojtan–Ursenbacher–Thome flow pattern map in order to develop the two-phase frictional pressure drop model based on flow pattern map, the new model is introduced and the development procedure is detailed. Comparisons with the database show that the new model is able to accurately and reliably predict experimental values and, furthermore, the variation of the frictional pressure drop vs. vapor quality is well captured.

The present work completes the fourth basic step in LTCM's flow pattern based work on obtaining a unified approach to modelling two-phase flow and heat transfer inside horizontal round tubes: (i) a generalized flow pattern map, (ii) a flow boiling heat transfer model, (iii) a convective condensation model and (iv) a two-phase frictional pressure drop model.

Acknowledgements

The project has been supported financially by the Fond National Swiss (FNS) Contract No. 21-57210.99 and by the Air-Conditioning and Refrigeration Technology Institute (ARTI) Contract No. 605-20040, which are gratefully acknowledged.

References

Bandel, J., 1973. Druckverlust und wärmeügang bei der verdampfung siedender kältemittel im durchströmten waagerechten rohr. Ph.D. thesis, University of Karlsruhe.

Bankoff, S.G., 1960. A variable density single-fluid model two-phase flow with particular reference to steam-water. J. Heat Transf. 11 (Series B), 265–272.

Baroczy, C.J., 1965. A systematic correlation for two-phase pressure drop. Chem. Eng. Prog. Symp. Ser. 62 (44), 232–249.

Beattie, D.R.H., 1972. Two-phase flow structure and mixing length theory. Nucl. Eng. Des. 21, 46–64.

Biberg, D., 1999. An explcit equation for the wetted angle in two-phase stratified pipe flow. Can. J. Chem. Eng. 77, 1221–1224.

Chawla, J.M., 1967. Wärmeübergang and druckfall in waagerechten rohren bei der strömung von verdampfenden kältemitteln. 523. VDI-Forschungsh, Ch. Lg1-Lg2.

Chisholm, D., 1973. Pressure gradients due to friction during the flow of evaporating two-phase mixtures in smooth tubes and channels. Int. J. Heat Mass Transf. 16, 347–358.

Cicchitti, A., Lombardi, C., Silvestri, M., Zavattarelli, G.S.R., 1960. Two-phase cooling experiments – pressure drop, heat transfer and burnout measurements. Energ. Nucl. 7 (6), 407–425.

el Hajal, J., Thome, J.R., Cavallini, A., 2003a. Condensation in horizontal tubes, part 1: two-phase flow pattern map. Int. J. Heat Mass Transf. 46, 3349–3363.

el Hajal, J., Thome, J.R., Cavallini, A., 2003b. Condensation in horizontal tubes, part 2: new heat transfer model based on flow regimes. Int. J. Heat Mass Transf. 46, 3365–3387.

Friedel, L., 1979. Improved friction drop correlations for horizontal and vertical two-phase pipe flow. In: European Two-phase Flow Group Meeting, paper E2. Ispra, Italy.

Grönnerud, R., 1979. Investigation of liquid hold-up, flow-resistance and heat transfer in circulation type of evaporators, Part iv: two-phase flow resistance in boiling refrigerans. In: Annexe 1972-1, Bull. de l'Inst. du Froid.

Hart, J., Hamersma, P.J., Fortuin, J.M.H., 1989. Correlations predcting frictional presure drop and liquid holdup during horizontal gas-liquid pipe flow with a small liquid holdup. Int. J. Multiphase Flow 15 (6), 947–964.

Hashizume, K., Ogiwara, H., Taniguchi, H., 1985. Flow pattern, void fraction and pressure drop of refrigerant two-phase flow in a horizontal pipe – II: analysis of frictional pressure drop. Int. J. Multiphase Flow 11, 643–658.

Kattan, N., Thome, J.R., Favrat, D., 1998. Flow boiling in horizontal tubes: Part 3 – development of a new heat transfer model based on flow pattern. J. Heat Transf. 120, 156–165.

Lockhart, R.W., Martinelli, R.C., 1949. Proposed correlation of data for isothermal two-phase, two-component in pipes. Chem. Eng. Proce. 45 (1), 39–48.

Moreno Quibén, J., 2005. Experimental and analytical study of two-phase pressure drops during evaporation in horizontal tubes. Thesis no 3337, Swiss Federal Institute of Technology Lausanne.

Müller-Steinhagen, H., Heck, K., 1986. A simple friction pressure correlation for two-phase flow in pipes. Chem. Eng. Proce. 20, 297–308.

Olujić, Z., 1985. Predicting two-phase flow friction loss in horizonta pipes. Chem. Eng. 24 (June), 45–50.

Ould-Didi, M.B., Kattan, N., Thome, J.R., 2002. Prediction of two-phase pressure gradients of refrigerants in horizontal tubes. Int. J. Refrig. 25, 935–947.

Pierre, B., 1964. Flow resistance with boiling refrigerants – Part 1. ASHRAE J. 6 (9), 58–65.

Rouhani, S.Z., Axelsson, E., 1970. Calculation of void volume fraction in the subcooled and quality boiling regions. Int. J. Heat Mass Transf 13, 383–393.

Steiner, D., 1993. VDI-Wärmeatlas (VDI Heat Atlas). Verein Deutscher Ingenieure VDI-Gessellschaft Verfahrenstechnik und Chemieingenieurwessen (GCV), Düsseldorf, Ch. Hbb.

Thom, J.R.S., 1964. Prediction of pressure drop during forced circulation boiling of water. Int. J. Heat Mass Transf. 7, 709–724.

Tribbe, C., Müller-Steinhagen, H.M., 2000. An evaluation of the performance of phenomenological models for predicting pressure gradient during gas–liquid flow in horizontal pipelines. Int. J. Multiphase Flow 26, 1019–1036.

Wojtan, L., 2004. Experimental and analytical investigation of void fraction and heat transfer during evaporation in horizontal tubes. Thesis no 2978, Swiss Federal Institute of Technology Lausanne.

Wojtan, L., Ursenbacher, T., Thome, J.R., 2005a. Investigation of flow boiling in horizontal tubes: Part I – A new diabatic two-phase flow pattern map. Int. J. Heat Mass Transf. 48, 2955–2969.

Wojtan, L., Ursenbacher, T., Thome, J.R., 2005b. Investigation of flow boiling in horizontal tubes: Part II – development of a new heat transfer model for stratified-wavy, dryout and mist flow regimes. Int. J. Heat Mass Transf. 48, 2970–2985.